ISSN 1070-3284, Russian Journal of Coordination Chemistry, 2017, Vol. 43, No. 2, pp. 133–137. © Pleiades Publishing, Ltd., 2017.

A Combination of Experiment and Molecular Simulation Studies on a New Metal-Organic Framework Showing pH-Triggered Drug Release[1]

F. M. Wang[a], J. Wang[b], **, S. Z. Yang[c], C. Y. Gu[c], X. R. Wu[c], *, J. Q. Liu[c], H. Sakiyama[d], J. W. Xu[c], M. M. Luo[c], and W. C. Liu[c]

[a] *Department of Chemistry and Chemical Engineering, Shaanxi Xueqian Normal University, Xian, P.R. China*

[b] *School of Chemistry and Environmental Engineering, Sichuan University of Science and Engineering, Zigong, 643000 P.R. China*

[c] *School of Pharmacy, Guangdong Medical University, Dongguan, 523808 P.R. China*

[d] *Department of Material and Biological Chemistry, Faculty of Science, Yamagata University, Kojirakawa, Yamagata, 990-8560 Japan*

**e-mail: scwangjun2011@126.com*

***e-mail: xirenwu@163.com*

Received January 11, 2016

Abstract—A new Co(II)-based complex $\{[Co_2(L)(4,4'\text{-Bipy})_2] \cdot CH_3CN\}_n$ (**I**) (H_4L = 5,5'-(biphenyl-4,4'-diyl-bis(methylene))bis(oxy)diisophthalic acid, 4,4'-Bipy = 4,4'-bipyridine) has been synthesized and structurally characterized. Single-crystal X-ray analysis (CIF file CCDC no. 1406388) reveals that compound **I** has 3D pcu topology. The incorporation of the drug 5-fluorouracil (5-FU) into the desolvated **I** was around 15.0 wt % of dehydrated **I**. Complex **I** also shows a pH-triggered controlled drug release property. In addition, we used semiempirical AM1 method to investigate the adsorption of 5-FU to **I** at the molecular level.

Keywords: drug delivery, release, structure

DOI: 10.1134/S1070328417020099

INTRODUCTION

The encapsulation and controlled release of active pharmaceutical ingredients is a critical factor in the development of optimal drug delivery systems [1, 2]. The unique characteristics of metal-organic frameworks [MOFs] are candidates for biological and medical applications. Potential adsorption and release properties of some drugs on MOFs were first described in [3]. A Pt-based drug at the nanoscale by using it as one building block to create a new coordination polymer were constructed in [4]. It was also reported that porous MOFs can adsorb and release several drugs, acting as a promising non-toxic drug carrier [5].

Until now, one of the most active fields for drug delivery systems is in the capability to load and release drugs in an acidic environment [6]. As pH in areas of tumor tissue is known to be more acidic than in normal tissue (pH 7.4) we can control the pH-responsive drug carrier to reduce undesired drug release during drug transportation and enhance the effective release of the anti-tumor drug in the tumor tissue, in which will reduce the adverse effects. Some examples of pH-sensitive drug loading materials have been succeeded to target cancer cells [7, 8]. However, it is still a challenge to explore a new carrier with high drug capacity and physiopathological pH signals to trigger selective drug release in targeted tissues [9–12].

After carefully consideration, herein, we chose the tetracarboxylate ligand 5,5'-(biphenyl-4,4'-diyl-bis(methylene))bis(oxy)diisophthalic acid (H_4L) with cobalt salt and 4,4'-bipyridine (4,4'-Bipy) to construct a 3D net with pcu topology based on dinulcear unit. Complex $\{[Co_2(L)(4,4'\text{-Bipy})_2] \cdot CH_3CN\}_n$ (**I**) synthesized by us has this structure. The incorporation of the drug 5-FU into the desolvated **I** was around 15.0 wt % per gram of dehydrated **I**. However, we present sustained drug release from desolvated **I** and its response to physiopathological pH signals.

EXPERIMENTAL

Materials and methods. All chemicals were purchased from Jinan Henghua Sci. and Tec. Co. Ltd. without further purification. IR spectra were recorded with a Perkin–Elmer Spectrum One spectrometer in

[1] The article is published in the original.

Table 1. Crystallographic data and structure refinement information for compound **I**

Parameter	Value
Formula weight	1023.73
Temperature, K	293
Crystal system	Orthorhombic
Space group	*Pbam*
Crystal color	Pink
a, Å	15.8306(11)
b, Å	16.3595(11)
c, Å	11.3985(8)
V, Å ^{3}	2952.0(4)
Z	2
ρ_{calcd}, g/cm^3	1.152
$F(000)$	1050
μ, mm^{-1}	0.615
θ Range, deg	2.49–24.85
Limiting indices hkl	$-20 \le h \le 18$, $-15 \le k \le 21$, $-14 \le l \le 14$
Reflections collected/unique (R_{int})	17480/580 (0.0313)
GOOF	1.055
R_1, wR_2 ($I > 2\sigma(I)$)*	0.0569, 0.1683
R_1, wR_2 (all data)**	0.0691, 0.1790
Large diff. peak and hole, e Å^{-3}	0.592 and −0.526

* $R = \Sigma(F_o - F_c)/\Sigma(F_o)$.

** $wR_2 = \{\Sigma[w(F_o^2 - F_c^2)^2]/\Sigma(F_o^2)^2\}^{1/2}$.

the region 4000–400 cm^{-1} using KBr pellets. Thermogravimetric analysis (TGA) was carried out with a Metter–Toledo TA 50 under dry dinitrogen flux (60 mL min^{-1}) at a heating rate of 5 K/min. X-ray powder diffraction (XRPD) data were recorded on a Rigaku RU200 diffractometer at 60 kV, 300 mA for CuK_α radiation (λ = 1.5406 Å), with a scan speed of 2 K/min and a step size of 0.02° in 2θ. An optimization by semiempirical AM1 method was made using MOPAC2012 program [13] and Winmostar software [14].

X-ray crystallography. Room-temperature X-ray diffraction measurements were carried out on a Bruker SMART APEX diffractometer that was equipped with a graphite monochromated MoK_α radiation (λ = 0.71073 Å) by using an ω-scan technique. The intensities were corrected absorption effects by using SADABS. The structures were solved by using SHELXS-97 and refined by using SHELX-97 [15]. Absorption corrections applied by using multi-non-hydrogen atoms were refined anisotropically. For **I**, the unit cell exhibits large regions that are occupied by solvent molecules; the solvent molecules could not be modeled. The SQUEEZE option in PLATON [16] was used to produce a set of solvent-free diffraction intensities. The nature and number of solvent molecules were established from CH&N elemental analyses and thermogravimetric analyses. Crystallographic details are given in Table 1. Selected bond dimensions are listed in Table 2.

Supplementary material for structure **I** has been deposited with the Cambridge Crystallographic Data Centre (CCDC no. 1406388; deposit@ccdc.cam.ac.uk or http://www.ccdc.cam.ac.uk).

Synthesis of complex I. A mixture of H_4L (27 mg, 0.05 mmol), Bipy (19 mg, 0.1 mmol), $Co(OAc)_2 \cdot 4H_2O$ (38 mg, 0.015 mmol) and H_2O (5 mL) and CH_3CN (3 mL) were placed in a Parr Teflon-lined stainless steel vessel (23 mL) and heated at 160°C for

Table 2. Selected bond distances (Å) and angles (deg) of structure **I**

Bond	d, Å	Bond	d, Å
Co(1)–O(4)	2.005(3)	Co(1)–O(3)	2.041(3)
Co(1)–O(1)	2.123(3)	Co(1)–N(1)	2.158(4)
Co(1)–O(2)	2.273(3)		
Angle	**ω, deg**	**Angle**	**ω, deg**
O(4)Co(1)O(3)	117.34(11)	O(4)Co(1)O(1)	152.44(11)
O(3)Co(1)O(1)	90.22(10)	O(4)Co(1)N(1)	88.4(2)
O(3)Co(1)N(1)	90.6(2)	O(1)Co(1)N(1)	91.48(19)
O(4)Co(1)O(2)	93.26(11)	O(3)Co(1)O(2)	149.40(10)

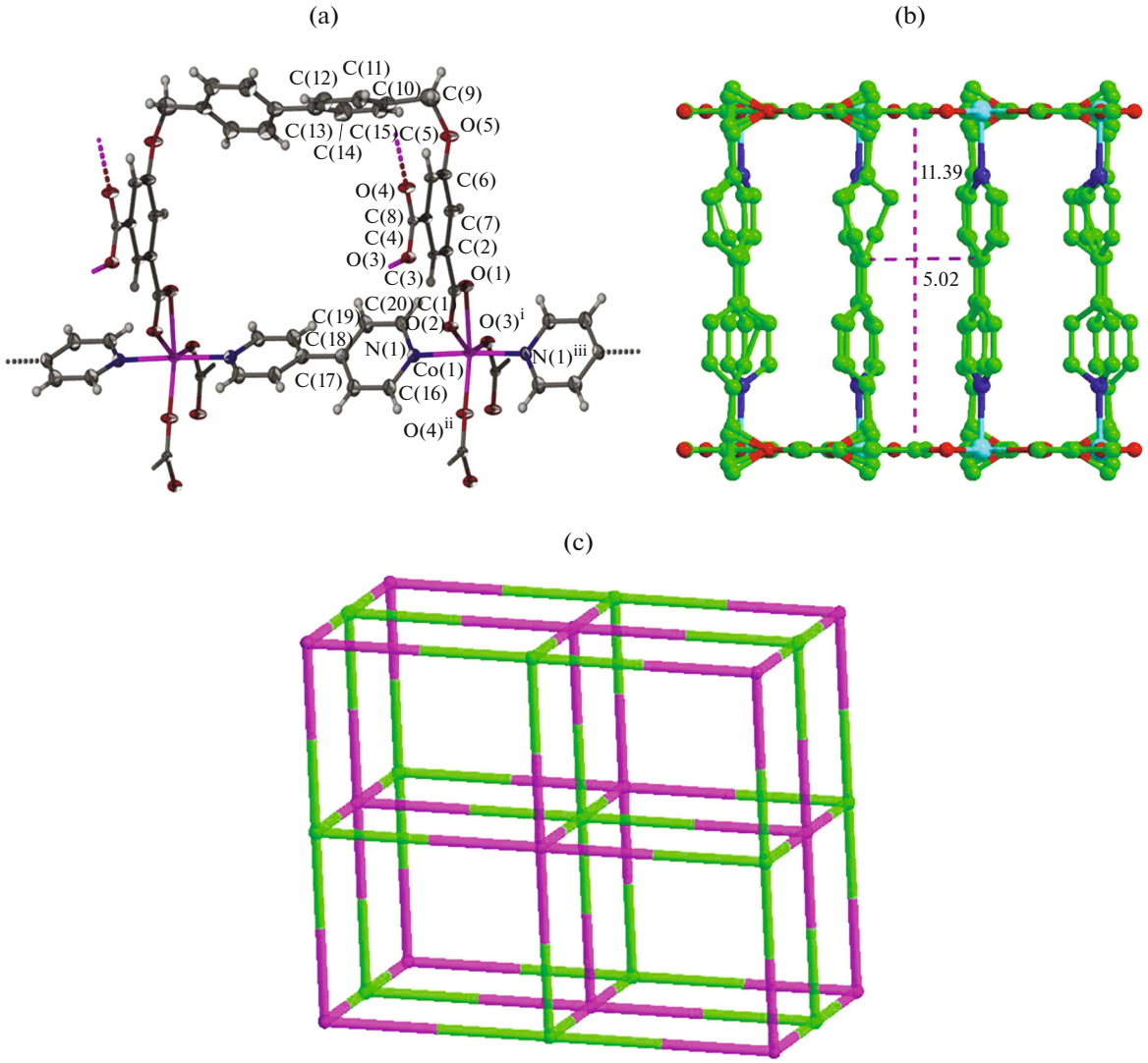

Fig. 1. Coordinative geometries of metal center and ligands (symmetric codes: [i] *x, y, z*; [ii] *–x, –y, z*; [iii] *–x, –y, –z* (a); view of the 3D network (b) and the schematic of pcu-like topology in **I** (c).

3 days. After the mixture was slowly cooled to room temperature, pink crystals were obtained.

For $C_{52}H_{37}N_6O_{10}Co_2$ (M = 1023.73)

anal. calcd., %:	C, 61.00;	H, 3.64;	N, 8.21.
Found, %:	C, 61.05;	H, 3.50;	N, 8.29.

IR (KBr; ν, cm^{-1}): 3420 m, 2917 w, 2358 m, 1629 v, 1537 v, 1438 v, 1388 m, 1034 m, 801 m, 723 m.

RESULTS AND DISCUSSION

The structure of **I** contains one unique Co atom, a half L ligand, one 4,4'-Bipy ligand, and intercalated CH_3CN molecules (all of which are related by symmetry). The $\{CoO_4N_2\}$ coordination spheres are each defined by two oxygen atoms from one chelating L carboxylate, two oxygen atoms from two different bidentate-bridging carboxylate groups, and two *cis*-oriented 4,4'-Bipy nitrogen donors (Fig. 1a). These Co dimers are connected to other dimers by the L ligand bridges. Each L bridge bonds to two Co atoms through one carboxylate group to form a dimer, and then to a third Co atom, which is part of another dimer, through the other chelating carboxylate group. Based on this connection, the dimers thus act as a 4-connecting node to generate a layer formed of a series of squares. These sheets are then bridged by the 4,4'-Bipy ligands to generate a 3D network. Each Co dimer is bridged to a dimer in the sheet above and below by pairs of 4,4'-Bipy ligands (Fig. 1b). If each pair is treated as a single link, the dimmers become 6-connecting nodes, and the overall topology is that of a pcu net (Fig. 1c) [17].

This compound has a building-like structure along the *z* axis. There is no hole on the *xy* plane floor, and

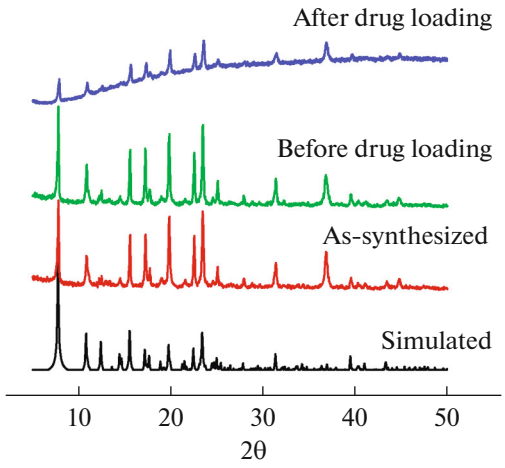

Fig. 2. Comparison of XRPD patterns of the simulated pattern from the single-crystal structure determination, the as-synthesized product, the desolvated and released phases in compound **I**.

between the floors, there are slender walls of pyridine and biphenyl groups. When we see the structure along the *z* axis, removing the ceiling, there are many small rooms surrounded by three bipyridine walls and three biphenyl walls. It should be emphasized that the probability of the bipyridine walls are 100%, but the probability of the biphenyl walls are 50%, due to the disorder. So, if half of the disordered groups are eliminated considering the steric repulsion, a zig-zag pore appears in the direction of the *x* axis.

FT-IR spectrum confirms incorporation of the drug molecule during adsorption process with presence of ν(C–H) at 2800 cm^{-1} and vibration bands characteristic of the carboxylate groups between 1620 and 1330 cm^{-1}. The characteristic peaks of 5-FU observed at 1700 and 1240 cm^{-1} were assigned to the stretching vibration of C=O and C–N groups, respectively. And the absorption bands of C–F deformation were also found at the 820–580 cm^{-1} region [18].

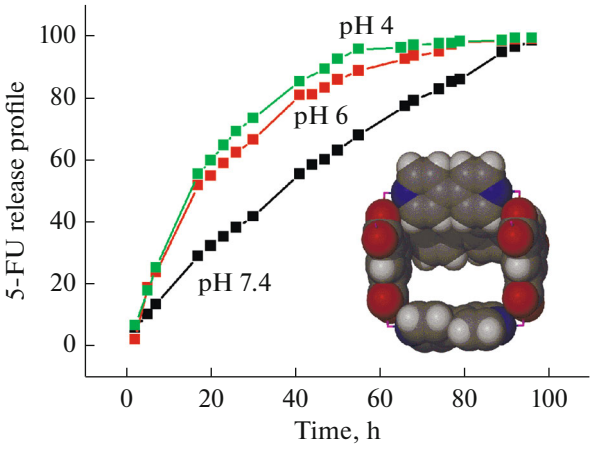

Fig. 3. 5-FU delivery (% 5-FU vs. time) from title compound and schematic illustration shows the drug 5-FU load and release process at different media.

To evaluate the capacity as drug delivery carriers of **I**, adsorption of anticancer 5-FU was carried by impregnating **I** under stirring in 5-FU containing ethanol solutions. Complex **I** was desolvated overnight prior to inclusion of the drug. As evidenced by XRPD, 5-FU content maintains its crystallinity (Fig. 2).

Complex **I** was desolvated at 120°C for 12 h prior to insertion of the drug. Crystallinity and incorporation of the drug molecule of **I** during adsorption process are confirmed by TGA and IR [19, 20]. To reach a maximal drug loading, 5-FU to porous solid relative ratio and contact time were tested. After the trivial tests, the best results were achieved when **I'** (**I'** is assigned as desolvated **I**) was soaked for 2 days in a 20 mL ethanol solution with a 5-FU to **I'** weight ratio of 1 : 2. This was confirmed by N_2 adsorption analyses showing that the surface area significantly decease upon drug molecules loading. It showed remarkable 5-FU adsorption and the loading content was measured to be 15.0%. This result is very lower than that of Cu(pi)-PEG5k polymer reported in [21]. As mentioned above, only one size of nanoscale cage (Fig. 1b) exists in **I** and the window is little match of the size of the drug molecule (5.3 × 5.0 Å). Therefore, it can be concluded that the some of total pore volume has not been used for occupying by drug molecules [19].

To investigate the pH-responsive drug release feature of **I**, release experiments were performed in phosphate buffer solution (PBS) (pH 7.4), phosphate buffer (pH 6.0 and 4.0) at 37°C. As shown in Fig. 3, 5-FU in **I** shows a slow release in PBS (pH 7.4) and approximately 35% of the drug was released at the early 24 h, then a stable release was observed during next 48 h. In contrast, the 5-FU release rate was markedly increased in PBS (pH 6.0 and pH 4.0). More then 55% of 5-FU released around 24 h, and then a plateau within 72 h was observed. These results imply that the loss of drug from **I** could be reduced during blood circulation; however, the drug release rate is accelerated after release into cancer cells. Thus, the loading drug may be effectively delivered into tumor tissues and cancer cells which may reduce side effects [21–23].

In order to find how fluorouracil (5-FU) molecules are taken into the pore, computational simulation was conducted based on the semi-empirical AM1 method. As a result, 5-FU molecules tended to interact with carboxylate oxygen atoms on the floor through hydrogen-bonding. Consequently, two 5-FU molecules were found to be incorporated in the unit cell (Fig. 4). Note that it is one of the probable structures. In the unit cell, **I** incorporates two 5-FU molecules instead of two acetonitrile molecules. That is, 1.00 g of the initial compound incorporates 0.127 g of 5-FU. It should be mentioned that the calculated loading value is little lower than the experimentally measured one. The discrepancy between calculated

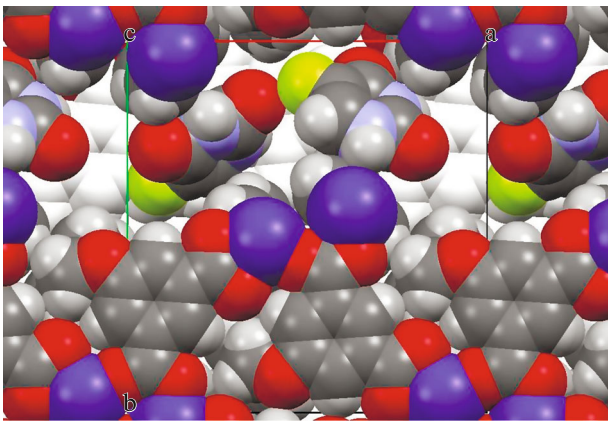

Fig. 4. 5-FU molecules incorporated in a pore, projected along the *z* axis.

and experimental values of drug loading can be caused by dynamics issues existent in the filling process such as diffusion, which cannot be captured directly from simulations. It can also originate from the experimental loading measurements, which are made indirectly from the excess of drug in solution. This protocol assumption (e.g., drug solubility, porous material activation and solvent-drug competition for binding sites in the material) are not easily ascertained.

ACKNOWLEDGMENTS

This work was partially supported by the grants from Shaanxi preschool teachers college high-level talent introduction start-up fund scientific research projects (2014DS020), Innovation Training Project of Guangdong Medical University (2015ZYDM015, 2015ZZDM007, 2015ZYDM005, 2014ZYDM017, 2014ZYDM018, and 2014ZZDM001), College Students Innovation Training Project of Guangdong Province (201510571054, 201510571048, 201510571076, 201410571060, and 201410571053), and thanks for prof. M. Zeller for refinement of structural data prof. Seik Weng Ng.

REFERENCES

1. Ananthoji, R., Eubank, J.F., Nouar, F., et al., *J. Mater. Chem.*, 2011, vol. 21, p. 9587.
2. Morris, R.E. and Wheatley, P.S., *Angew. Chem. Int. Ed.*, 2008, vol. 47, p. 4966.
3. Horcajada, P., Chalati, T., Serre, C., et al., *Nat. Mater.*, 2010, vol. 9, p. 172.
4. Taylor-Fashow, K.M.L., Rocca, J.D., Xie, Z.G., et al., 2009, vol. 131, p. 14261.
5. Horcajada, P., Gref, R., Baati, T., et al., *Chem. Rev.*, 2011, vol. 112, p. 1232.
6. Little, S.R., Lynn, D.M., and Ge, Q., *Proc. Natl. Acad. Sci. U.S.A.*, 2004, vol. 101, p. 9534.
7. Wang, C., Ge, Q., Ting, D., et al., *Nat. Mater.*, 2004, vol. 3, p. 190.
8. Jung, J., Lee, I.-H., Lee, E., et al., *Biomacromolecules*, 2007, vol. 8, p. 3401.
9. Yang, X.Y., Wang, Y.S., Huang, X., et al., *J. Mater. Chem.*, 2011, vol. 21, p. 3448.
10. Chalati, T., Horcajada, P., et al., *Nanomedicine*, 2011, vol. 6, p. 1683.
11. Horcajada, P., Serre, C., Vallet-Regi, M., et al., *Agnew. Chem. Int. Ed.*, 2006, vol. 45, p. 5974.
12. Bernini, M.C., Fairen-Jimenez, D., Pasinetti, M., et al., *J. Mater. Chem. B*, 2014, vol. 2, p. 766.
13. Stewart, J.J.P., *MOPAC2012*, http://openmopac.net/MOPAC2012.html
14. Senda, N., *Winmostar*, 2008. http://winmostar.com
15. Sheldrick, G.M., *Acta Crystallogr., Sect. A: Found. Crystallogr.*, 2008, vol. 64, p. 112.
16. Spek, A.L., *J. Appl. Crystallogr.*, 2015, vol. 71, p. 9.
17. Ma, L.F., Qin, J.H., Han, M.L., et al., *Inorg. Chem. Commun.*, 2011, vol. 14, p. 1584.
18. Férey, G., Mellot-Draznieks, C., Serre, C., and Millange, F., *Acc. Chem. Res.*, 2005, vol. 38, p. 217.
19. Zhang, Z.H., Chen, S.C., Chen, Q., et al., *Inorg. Chem. Commun.*, 2011, vol. 14, p. 1819.
20. Horcajada, P., Surblé, S., Serre, C., et al., *Chem. Commun.*, 2007, vol. 27, p. 2820.
21. Zhao, D., Tan, S.W., Yuan, D.Q., et al., *Adv. Mater.*, 2011, vol. 23, p. 90.
22. Zhuang, J., Kuo, C.H., Chou, L.Y., et al., *ACS Nano*, 2014, vol. 8, p. 2812.
23. Sun, C.Y., Qin, C., Wang, X.L., et al., *Dalton Trans.*, 2012, vol. 41, p. 6906.